



1 **Measurement Report: A Multi-Year Study on the Impacts of Chinese New Year Celebrations on Air**
2 **Quality in Beijing, China.**

3
4 Benjamin Foreback^{1,2}, Lubna Dada², Kaspar Dällenbach², Chao Yan^{1,2}, Lili Wang³, Biwu Chu^{2,4}, Ying Zhou¹,
5 Tom V. Kokkonen^{2,6}, Mona Kurppa⁷, Rosaria E. Pileci⁵, Yonghong Wang², Tommy Chan², Juha
6 Kangasluoma^{1,2}, Lin Zhuohui¹, Yishou Guo¹, Chang Li¹, Rima Baalbaki², Joni Kujansuu^{1,2}, Xiaolong Fan¹,
7 Zemin Feng¹, Pekka Rantala², Shahzad Gani², Federico Bianchi^{1,2}, Veli-Matti Kerminen², Tuukka Petäjä^{1,2,6},
8 Markku Kulmala^{1,2,6}, Yongchun Liu¹ and Pauli Paasonen^{1,2}

9
10 ¹Aerosol and Haze Laboratory, Beijing Advanced Innovation Center for Soft Matter Science and Engineering,
11 Beijing University of Chemical Technology, Beijing, China

12 ²Institute for Atmospheric and Earth System Research / Physics, Faculty of Science, University of Helsinki,
13 Finland

14 ³Institute of Atmospheric Physics, Chinese Academy of Sciences, Beijing, China

15 ⁴ State Key Joint Laboratory of Environment Simulation and Pollution Control, Research Center for Eco-
16 Environmental Sciences, Chinese Academy of Sciences, Beijing 100085, China

17 ⁵Laboratory of Atmospheric Chemistry, Paul Scherrer Institute (PSI), 5232 Villigen, Switzerland

18 ⁶Joint International Research Laboratory of Atmospheric and Earth System Sciences, School of Atmospheric
19 Sciences, Nanjing University, Nanjing, China

20 ⁷Atmospheric Composition Research, Finnish Meteorological Institute, Helsinki, Finland

21
22 Corresponding Author: Pauli Paasonen (pauli.paasonen@helsinki.fi)

23
24
25 **ABSTRACT**

26 We investigated the influence of the Chinese New Year (CNY) celebrations on local air quality in Beijing from
27 2013 through 2019, bringing together comprehensive observations at the newly-constructed Aerosol and Haze
28 Laboratory at Beijing University of Chemical Technology – West Campus (BUCT-AHL) and data from
29 Chinese government air quality measurement stations. In this study, these datasets are used together to provide
30 a detailed analysis of air quality during the CNY over multiple years. Before CNY in 2018, the city of Beijing
31 prohibited the use of fireworks and firecrackers in an effort to reduce air pollution. In 2018 air pollutant
32 concentrations still showed a significant peak during the CNY night, even though not as strong as in previous
33 years, but in 2019, the pollution levels were notably lower. During the studied 7-year study period, it appears
34 that there has been a long-term decrease in CNY related emissions since 2016. Based on our analysis, the
35 pollutants with the most notable spike during CNY were sulfur dioxide and particulate matter, including black
36 carbon. Sulfuric acid concentration followed the sulfur dioxide concentration and showed elevated overnight
37 concentration in CNY 2018, but not notably in 2019. Additionally, spectrometer data and analysis of aerosol
38 particle number size distribution shows direct emissions of particles with diameters around 20 nm during CNY
39 in 2018 and 2019. Meteorological conditions were comparable between the latest two years, indicating that air
40 quality associated with the CNY may be improving, perhaps a positive effect of the restrictions. The longer
41 observations in the future will provide confirmation for these trends.

42
43 **1 INTRODUCTION**

44
45 Anthropogenic emissions associated with festivities, notably fireworks and firecrackers (hereafter simply
46 fireworks), are known for their hazardous effects, and even short-term exposure can have significant impacts
47 on human health (Bach et al., 2007; Chen et al. 2011; Jiang et al. 2015; Yang et al. 2014). Firework celebrations



48 are found to increase the concentrations of trace gases and particle concentrations (Kong et al. 2015; Li et al.
49 2013). Furthermore, some studies have related these festivities to the occurrence of haze episodes in the days
50 following a firework event (Li et al. 2013; Feng et al. 2012).

51

52 The CNY is a traditional annual holiday occurring in wintertime – in January or February (the exact date is
53 based on the lunar cycle). Because of the adverse impacts on health, pollution from fireworks during the CNY
54 has gathered attention worldwide. For instance, studies including Yang et al. (2014) in Jinan, Shi et al. (2014)
55 in Tianjin, and Feng et al. (2012) and Zhang et al. (2010) in Shanghai have shown that there is noticeable
56 degradation in air quality associated with Chinese New Year celebrations in these cities. The effects of
57 fireworks on air pollution are known for various holidays in other countries as well. Studies in India, for
58 example, during the country's annual Diwali Festival in the late autumn have also shown results of high
59 pollution from firework use (Ravindra et al. 2003; Mönkkönen et al. 2004; Barman et al. 2007; Singh et al.
60 2009; Yerramesetti et al. 2013). As another example, a study by Liu et al. (1997) in Southern California, USA
61 showed enhanced concentrations of particulate matter and trace gas pollutants during firework celebrations.

62

63 Beginning in 2018, a prohibition on firework burning within the 5th Ring Road of Beijing was implemented
64 (Liu et al. 2019). The study by Liu et al. (2019) reported that the prohibition resulted in about a 40% decrease
65 in the total number of fireworks and firecrackers sold in Beijing around the 2018 CNY compared to 2016.
66 Furthermore, the amount of toxic pollution during the 2018 CNY was significantly less than that in 2016.

67

68 In this study, we focus on the measurements collected from the Beijing University of Chemical Technology,
69 Aerosol and Haze Laboratory (BUCT-AHL, Liu et al., 2020), an academic research station in Beijing China,
70 along with seven years of data from the Chinese Ministry of Environmental Protection (MEP) throughout the
71 Beijing metropolitan area. The long-term datasets also provide spatial context in the scale of the greater Beijing
72 area, including a comparison of measurements inside versus outside of the prohibition area. Here we
73 investigated years 2013-2019. The 2020 CNY has not been included in this study because of the widespread
74 impacts of the COVID-19 virus that affected China during this time. Due to the unfortunate circumstance, many
75 Chinese citizens refrained from travel, public celebrations, and time spent in public. Consequently, the 2020
76 CNY is not directly comparable to previous years.

77

78 The aim of this this paper is to provide a detailed view on how CNY celebrations have influenced air quality,
79 atmospheric chemistry and gas-to-particle conversion in Beijing. We start with an in-depth analysis of data
80 from 2018 and 2019 while the longer, 7-year data set provides the perspective into the impacts of the imposed
81 restrictions on firework use in the Beijing area. The specific questions we aim to answer include: i) how do the
82 CNY celebrations and associated increase in precursor and aerosol emissions reflect into the atmospheric
83 concentrations of trace gases and particulate matter and particle number size distribution; ii) how are these
84 changes connected with meteorological conditions; iii) how does the influence of CNY to regional air quality
85 vary spatially over the Beijing area; iv) how the influence of CNY on Beijing air quality has changed during
86 the recent years, including the result of the firework prohibition beginning in 2018; and v) how does the gas
87 phase sulfuric acid relate to the new particle formation and cluster mode particle number concentration during
88 CNY. Our insights are useful for scientists and policy makers around the world who are interested in improving
89 air quality during holidays that involve firework celebrations. Improving air quality, even short-term, could
90 have a significant positive impact on health and wellbeing of citizens.

91

92 **2 METHODS**

93

94 **2.1 Measurement sites**

95



96 Data collected for this study have been measured at the newly constructed station near the third ring road of
97 Beijing (39°56'N, 116°17'E; Figure 1, Liu et al., 2020). The station, known as the Aerosol and Haze Laboratory,
98 is located on Beijing University of Chemical Technology West Campus, which is a five-floor building nearby
99 to a busy highway. The station, hereafter BUCT-AHL, is following the concept of the Station for Measuring
100 Ecosystem-Atmosphere Relations (SMEAR) in Hyytiälä, Southern Finland (Hari and Kulmala, 2005). BUCT-
101 AHL was built in collaboration with the Institute of Atmospheric and Earth System Research (INAR) at the
102 University of Helsinki as part of the effort to build a global SMEAR network (Kulmala, 2018), with the aim to
103 understand atmospheric chemical cocktail in megacity (Kulmala, 2015).

104

105 In our analysis the following datasets from BUCT-AHL during the 2018 and 2019 CNY are used: 1) Trace gas
106 concentrations: nitrogen oxides (NO_x), sulfur dioxide (SO₂), ozone (O₃), and carbon monoxide (CO), 2) PM_{2.5}
107 aerosol mass concentration, 3) Black carbon mass concentration (BC), 4) Sub-micron aerosol particle number
108 size distributions, 5) Gas-phase sulfuric acid (H₂SO₄) concentration, 6) Meteorological observations.

109

110 Additionally, datasets from several national air quality monitoring sites (NAQMS; Song et al. 2017; Tao et al.
111 2016) within Beijing obtained from the Chinese Ministry of Environmental Protection (MEP) were utilized as
112 follows: 1) Fine and coarse particulate matter mass concentrations (PM_{2.5} and PM₁₀), 2) trace gases (NO_x,
113 SO₂, O₃, and CO) from 2013 through 2019 for a multi-year comparison. This also provided insights into the
114 spatial variability within the Beijing city and particularly contrasting the area, where the ban for the fireworks
115 was implemented against the urban background air quality.

116

117 **2.2 Instrumentation**

118

119 **2.2.1 Observations in BUCT-AHL station**

120

121 **Trace gas measurements**

122 Concentrations of carbon monoxide (CO), sulfur dioxide (SO₂), ozone (O₃) and nitrogen oxides (NO_x) were
123 measured with Thermo Environmental Instruments models 48i, 43i-TLE, 42i, and 49i, respectively. They were
124 all sampled through a common inlet through the roof of the building. The length of the sampling tube was
125 approximately 3 m long (Zhou et al. 2020). The time resolution of the measurements was 5 minutes, but to be
126 consistent with the MEP datasets, one hour averages were used in this study.

127

128 **Meteorological observations**

129 Meteorological datasets were collected with a Vaisala automatic weather station, AWS310 on the rooftop of
130 BUCT-AHL including wind speed and direction, ambient air temperature and relative humidity. Boundary
131 layer height was measured using a Vaisala CL-51 ceilometer on the rooftop of BUCT-AHL.

132

133 **Sub-micron aerosol particle number size distributions and total number concentrations**

134 Particle size distribution between 3 nm and 1 μm was measured using a particle size distribution (PSD) (Liu et
135 al., 2016). The PSD is composed of a nano-scanning mobility particle sizer (nano-SMPS, 3–55 nm, mobility
136 diameter), a long SMPS (25–650 nm, mobility diameter) and an aerodynamic particle sizer (APS, 0.55–10 μm,
137 aerodynamic diameter). It was fitted with a cyclone to remove particles larger than 10 μm from entering the
138 system. Sampling was done from the rooftop using a 3 m long sampling tube. Additional information about the
139 setup of these instruments can be found in Zhou et al. (2020).

140

141 Particle sizes have been further divided into four modes, based on particle diameter: cluster mode (sub-3 nm),
142 nucleation mode (3–25 nm), Aitken mode (25–100 nm), and accumulation mode (100–1000 nm). The method
143 of is described in Zhou et al. (2020).



144

145 Furthermore, at BUCT-AHL, aerosol particle number size distribution of aerosol particles from 2.5 to 42 nm
146 was measured with a neutral cluster and air ion spectrometer (NAIS; model 4-11, Airel, Estonia; Manninen et
147 al., 2016; Mirme and Mirme, 2013). The NAIS sampled outside air from a horizontally oriented, 4 cm diameter
148 copper sampling tube extending 1.6 m out of a north-facing window. The sampling flow rate was 54 l min^{-1}
149 (Zhou et al., 2020).

150

151 Additionally, an Airmodus A11 Nano Condensation Nucleus Counter (nCNC) system, commonly known as
152 PSM (Vanhanen et al., 2011) was used to measure the sub 3nm particle number concentration. The PSM was
153 operated in scanning mode in which the saturator flow is continuously ramped between 0.1 and 1.3 lpm and
154 back to 0.1 lpm. The sampling line was 1.2 m long and having the same orientation as the NAIS sampling line.

155

156 **Gas-phase sulfuric acid**

157 Sulfuric acid was measured by a chemical ionization atmospheric-pressure interface time-of-flight mass
158 spectrometer equipped with a nitrate chemical ionization source (CI-APi-TOF, Jokinen et al., 2012). The
159 ionization was done with NO_3^- as the reagent ion in ambient pressure (e.g., Petäjä et al., 2009). Nitrate reagent
160 ion was produced by photo-ionizing a mixture of $3 \text{ mL}\cdot\text{min}^{-1}$ ultrahigh purity nitrogen flow containing nitric
161 acid with $20 \text{ mL}\cdot\text{min}^{-1}$ zero air. This mixture acted as the sheath flow and was introduced into a coaxial laminar
162 flow reactor concentric to the sample flow. The sample flow was $8.8 \text{ L}\cdot\text{min}^{-1}$ but only $0.8 \text{ L}\cdot\text{min}^{-1}$ was drawn
163 into the pinhole of the TOF. The sampling line was 1.6 m long stainless-steel tube having an inner diameter of
164 $3/4$ inch and positioned horizontally. The instrument was calibrated with known concentrations of sulfuric acid.
165 Further information about the calibration procedure can be found in Kürten et al. 2012.

166

167 **Black carbon mass concentration**

168 An aethalometer AE33 (Magee Scientific) monitored the light absorption related to the aerosol. Equivalent
169 black carbon (eBC) was computed based on the change in time of the light attenuation using procedures
170 presented in Virkkula et al. (2015)

171

172 **2.2.2 Chinese MEP Data**

173 Beginning in 2013, the Chinese Ministry of Environmental Protection began installing sensors China-wide to
174 measure local, regional, and large-scale air quality. Real-time datasets from this sensor network are published
175 hourly by the China Environmental Monitoring Center (CEMC), which includes PM_{10} , $\text{PM}_{2.5}$, SO_2 , NO_x and
176 CO. There are over 1000 active sensors across China (Song et al. 2017; Tao et al. 2016).

177

178 In this study, data from 12 MEP sites throughout Beijing are used (See Table 1 in Supplementary Information
179 for a list of these sites and their locations). The Guanyuan (GY) site is the closest site to BUCT-AHL, about 5
180 km east. The original data are available at <http://106.37.208.233:20035/> and for this study we have removed
181 the outliers with criteria presented by Wu et al. (2018).

182 **3 RESULTS AND DISCUSSION**

183

184 Effects of elevated pollutant emissions during the Chinese New Year were observed both at BUCT-AHL and
185 the MEP sites during the analysis periods. Effects include sudden spikes in concentrations of trace gases,
186 particles, and BC. We explore the time series of the observations in the section below in more detail.

187

188 **3.1 Characteristics of air quality during the Chinese New Year**

189



190 Figure 2 shows a timeseries of air pollutant concentrations from eight days before to eight days after the 2018
191 and 2019 CNY at BUCT-AHL. The CNY was on February 16, 2018 and February 5, 2019. In the BUCT
192 measurements, we observed sharp peaks in Particulate Matter mass ($PM_{2.5}$), SO_2 , sulfuric acid, CO, BC, NO,
193 and NO_2 and ozone during firework events. These observations agree with the previous studies showing a
194 connection between holiday-related firework celebrations and degraded air quality (Jiang et al., 2015; Yang et
195 al., 2014; Shi et al., 2014; Feng et al., 2012; Zhang et al., 2010).

196
197 Figure 2 shows that in 2018, a significant spike in $PM_{2.5}$ concentration is observed overnight, in particular at
198 midnight, on the CNY. Additionally, in 2018 period of haze for three days following the CNY was observed.
199 In contrast, in 2019, $PM_{2.5}$ was observed to have lower concentration on the CNY night than on the previous
200 and following nights. There is also a noticeable spike in SO_2 overnight of the CNY in 2018, shown in Figure
201 3, but less noticeable alteration of SO_2 is observed overnight of the 2019 CNY.

202
203 The measurements show clearly elevated nighttime concentration of H_2SO_4 on CNY in 2018, concentration
204 exceeding $3 \times 10^6 \text{ cm}^{-3}$ during the whole night, whereas on other nights such high concentrations are observed
205 only occasionally. In 2019, there is no signs of anomalies in nighttime H_2SO_4 concentration during CNY. An
206 unknown spike in H_2SO_4 is noticed at noon the day before CNY in 2018, and its association with celebratory
207 activities is unclear. Like with $PM_{2.5}$ and SO_2 , Figure 2 shows a clearly distinctive spike in BC around midnight
208 of the 2018 CNY. However, there appears to be little to no effect of CNY on BC in 2019.

209
210 The measurements show elevated concentration of NO_2 overnight of the CNY in both years, yet no spike in
211 NO concentration. Fireworks emit NO_2 but not NO (Jiang et al., 2015); however, a high NO_2/NO_x ratio can
212 also be caused by accumulation of pollutants emitted the previous afternoon (Chou et al., 2009). Nonetheless,
213 when comparing the CNY characteristics of NO_x with other pollutants, there is a noticeable spike of NO_2 during
214 the CNY during both years.

215
216 Generally, Figure 2 shows that during the CNY celebrations in 2018 concentrations of all the primary pollutants
217 are elevated, implying enhanced direct emissions. The concentrations of sulfuric acid and ozone react to
218 elevated concentrations as expected, sulfuric acid concentration increases due to enhanced formation with
219 increased SO_2 concentration, and ozone concentration decreases with increased chemical sink by NO_x and CO
220 (and probably other carbon compounds). However, on 2019, only the concentrations of CO and NO_2 are
221 observed to increase during CNY celebrations, leading to decrease in ozone concentration, whereas the
222 concentrations of all other pollutants did not show elevated concentrations. Interestingly, the measurements in
223 Figure 2 show degraded air quality between 16-20 February 2018 immediately following the Chinese New
224 Year, which closely resembles the characteristics of a haze event as described in Zhao et al. (2013) and Zhao
225 et al. (2011). These haze events have elevated concentrations of pollution continuously for multiple days, and
226 these concentrations gradually increase throughout the episodes, and they end with sudden decline, often caused
227 by a cold front or synoptic weather system. Several previous studies, including Jiang et al. (2015) and Li et al.
228 (2013), suggest that fireworks likely contribute to haze formation. Therefore, the increased level of pollutants
229 observed overnight during the 2018 CNY have likely contributed to this subsequent haze period. However, the
230 meteorological conditions are also important for haze formation, which are discussed in Section 3.2.

231 232 **3.2 Effects of Meteorology and Boundary Layer Height** 233

234 Because meteorology conditions vary between different years, it is important to understand its effects on
235 pollution when comparing different years to each other. Most notably, wind, humidity, boundary layer height,
236 and precipitation can affect pollutant concentrations during and after the fireworks.

237



238 The wind speed during the night of the 2018 CNY peaks at ~ 2 m/s, whereas during the night of the 2019 CNY,
239 it remains less than ~ 1 m/s. Temperature and relative humidity are quite comparable between the years.
240 Precipitation was not measured at BUCT-AHL in either year. However, online weather data shows there was
241 no precipitation in the region during either of the years
242 (<https://www.wunderground.com/history/weekly/cn/beijing/ZBNY/date/2019-2-4>). The nocturnal boundary
243 layer heights are low in both years (Figure 2), which is unfavorable for vertical mixing of pollutants. This,
244 along with the low wind speeds, points towards more efficient dispersion in pollutant concentrations in 2018
245 than in 2019, indicating that the reason for clearly lower pollutant concentrations in 2019 is likely related to
246 lower emissions, not meteorological conditions.

247

248 3.3 Particle number concentrations and size distribution

249

250 To further explore the effects the fireworks on air pollution, Figure 3 shows particle number concentrations and
251 size distributions measured by the NAIS instrument at BUCT-AHL from the day before to the day after CNY.
252 The results show that shortly before midnight on CNY in 2018, an elevated concentration of aerosol particles
253 with diameters of roughly 20 nm was observed, simultaneous to the spike in SO_2 concentration. This increase
254 in particle number concentration is not associated with a regional new particle formation (NPF) event (e.g.
255 Mäkelä et al., 1997; Shen et al., 2011; Heintzenberg et al. 2007), which in this case is taking place on the
256 following day before noon, where the concentrations of well below 10 nm particles are first observed to increase
257 and then to grow to 20 nm sizes. This feature suggests that the observed particles during festivities are of
258 primary origin and emitted to atmosphere in the respective size range, possibly from the fireworks. Similar to
259 most other pollutants, particle number concentrations in this size range in CNY 2019 do not show signs of
260 celebration related emissions. There is a continuous concentration of particles in the respective size range, but
261 no clear peaks during the celebrations, in line with no signs of increased SO_2 concentration.

262

263 Aerosol particle mass concentration ($\text{PM}_{2.5}$) during the CNY firework period is clearly elevated reaching
264 values close to $250 \mu\text{g m}^{-3}$ and $150 \mu\text{g m}^{-3}$ at midnight for the year 2018 and 2019, respectively, which are
265 considerable higher than the mass concentrations on the previous day. The midnight peak in PM mass
266 concentration coincides with atmospheric nanoparticle concentrations and elevated SO_2 in 2018 indicating high
267 emissions of primary aerosol particles and co-emitted sulfur dioxide.

268

269 Figure 4 shows the particle number concentrations in four size modes, namely sub-3 nm cluster mode, 3-25 nm
270 nucleation mode, 25-100 nm Aitken mode, and 100-1000 nm accumulation mode, as a function $\text{PM}_{2.5}$
271 concentration measured at BUCT-AHL in 2018 and 2019, for 48 hours before through 48 hours after the CNY.
272 The darker colors mark the nighttime measurements on the CNY (9pm-5am). The night-time mass
273 concentrations are noticeably greater. The mass-to-number concentration comparison follows the same general
274 curve during nighttime as the full time period, and the pattern, including the nighttime observations, is
275 consistent with recent investigation by Zhou et al. (2020). The $\text{PM}_{2.5}$ concentrations during the CNY period in
276 2018 are significantly higher than in other periods. The cluster and nucleation mode concentrations are lower,
277 Aitken mode is on the same level, and accumulation mode concentration is higher during the CNY period. This
278 is reasonable, as accumulation mode particles contribute significantly to $\text{PM}_{2.5}$ mass and constitute the major
279 sink for cluster and nucleation mode particles due to coagulation scavenging of smaller particles by larger ones.

280

281 In figure 5 we can see how the cluster mode concentrations behaves as a function of sulfuric acid. The high
282 nocturnal sulfuric acid concentration during CNY celebrations in 2018 do not lead to high cluster or nucleation
283 mode concentration. In fact, the particle number concentrations in these modes deviates from the otherwise
284 clear response to sulfuric acid concentrations. The reason for this is visible in the panel for accumulation mode
285 concentration vs sulfuric acid concentration: during the CNY 2018 the high concentrations of accumulation



286 mode particles correlates with sulfuric acid concentration thus plausibly neglecting the enhanced particle cluster
287 and particle formation rates by enhanced coagulation sink as explained earlier.

288

289 **3.4 Multi-Year Variation of Chinese New Year Effects in Beijing**

290

291 Although fireworks were formally prohibited within the 5th Ring Road of Beijing beginning in 2018, there was
292 still evidence of fireworks burning either in the city or the immediate vicinity of the city, as measured at BUCT-
293 AHL, which is within the prohibition area. Nonetheless, because the initial peak during the 2018 CNY (Figure
294 6) is significantly higher, even though it disperses more quickly, it is therefore evident that there was more
295 initial pollution during this time, whereas the amount of pollution during the 2019 CNY was considerably less,
296 even though it remained present for longer time period.

297

298 A longer-term multi-year study can be useful in demonstrating whether or not the policy is effective in reducing
299 firework-related pollution, and if there is an overall decreasing trend of pollution effects from fireworks over
300 multiple years. To investigate this question, it is useful to compare the 2018 and 2019 CNY with previous years
301 in Beijing. Datasets have been analyzed from 12 stations in Beijing from 2013 through 2019.

302

303 Figure 6 shows that each year, there was a spike in pollution around midnight during the CNY. The highest
304 levels were observed in 2016, and the lowest levels were in 2019. Observations from 2013, 2014, 2015, and
305 2017 also showed similarly high or higher levels of PM_{2.5} as in 2018 (unfortunately the 2017 dataset is
306 incomplete and does not extend beyond 00:00 of New Year day). Furthermore, data from 2013, 2014, 2015
307 and 2018 suggest the presence of haze episodes in the days following the New Year, potentially related to
308 firework burning. An elevated level of pollution for two days after the CNY compared to before the CNY was
309 observed in 2019 as well, even though it was to a lesser extent.

310

311 Data from the CNYs have also been compiled into box plots in Figure 7, depicting the distributions of pollutant
312 concentrations from 6:00 pm on CNY Eve to 6:00 am on the CNY day each year. The highest PM
313 concentrations during this time were in 2016 and have since decreased. Concentrations of NO₂, SO₂, and CO
314 all show a similar pattern as PM. It should be noted that in 2017, the data is missing after midnight. The decrease
315 since 2016 agrees with the results obtained by Liu et al. 2019. Since ozone is a secondary product and it reacts
316 with several primary pollutants, its concentration pattern being roughly opposite to those of primary pollutants
317 is as expected. In this aspect, it is notable that in 2019 in addition to primary pollutant concentrations also ozone
318 concentration has decreased from 2017 and 2018.

319

320 **3.5 Spatial variability based on MEP measurement network data**

321

322 A further analysis of the CNY in Beijing is to perform a spatial comparison of the MEP measurements across
323 the Beijing region. This includes comparing the observations inside the 5th Ring Road, where fireworks were
324 prohibited, to outside the ring. Figure 8 maps the 12 MEP stations in the Beijing region for 2013-2019, showing
325 the relative difference of PM_{2.5} measurements from 9 pm through 5 am during the night of CNY to the average
326 of measurements \pm 48 hours of the CNY at each site. Figures in Supplementary Information show observations
327 of PM_{2.5} from the 12 individual MEP sites and the corresponding differences, year-by-year from 2013-2019.
328 Based on Figure 8, we can see significant variation from year to year as to which station measures the highest
329 pollution. It is important to note that the population density is greater closer to city center, and thus the
330 population density could impact the results. However, it is plausible to assume that the relative population
331 density difference between the city center and the surrounding areas do not change dramatically during the few
332 year time period.

333



334 Figure 8 illustrates that in 2013 and 2014, the enhancement in $PM_{2.5}$ concentrations during CNY is greater
335 inside the 5th ring than outside. In 2015, the enhancement is much greater at the two northeastern sites (HR and
336 SY). In 2016, the differences vary, with no clear difference inside or outside the 5th ring. In 2018, the
337 enhancement of $PM_{2.5}$ is higher inside the 5th ring than outside, except for the SY site to the far northeast, which
338 had significantly high enhancement compared to the other sites. In 2019 the enhancement is overall less inside
339 compared to outside.

340

341 Figure 9 shows differences between the $PM_{2.5}$ median of the sites inside the 5th Ring Road and the median of
342 the sites outside the 5th Ring (that is the median of the 8 inside sites minus the median of the outside 4 stations)
343 48 hours before through 48 hours after the CNY for 2013-2019. In most years, there is a greater enhancement
344 of $PM_{2.5}$ inside than outside. However, in 2015, the opposite was true. In 2016, the first part of the CNY
345 overnight had lower $PM_{2.5}$ inside than outside, but that reversed a few hours later. In 2019, there was less $PM_{2.5}$
346 inside than outside throughout the night of CNY.

347

348 4 CONCLUSIONS

349

350 This study confirms that CNY consistently impacts air quality in Beijing year-after-year. These results are
351 consistent with previous studies that have linked the CNY (and other similar holiday celebrations involving
352 firework burning around the world) to degraded air quality both locally and regionally. Our results suggest that
353 the regulations to limit firework use have improved the air quality within the restriction zone inside the fifth
354 ring road in Beijing since 2016.

355

356 Based on our observations at BUCT-AHL station in Beijing, in 2018, we detected clearly higher than typical
357 night-time concentrations of particulate mass ($PM_{2.5}$), particle number, trace gas and sulfuric acid
358 concentrations during the CNY. The increase in sulfuric acid concentration did not lead to observed new
359 particle formation, which is explained by simultaneously increasing condensation and coagulation sinks for
360 clustering vapors and freshly formed particles, respectively. However, we observed appearance of particles
361 with diameters of roughly 20 nm that seemed to be linked to enhanced sulfur dioxide concentrations. Based
362 on the MEP data, the peaks in concentrations of different pollutants were noticeably lower than in the previous
363 years. In 2019, a peak in pollution was observed overnight, but it was significantly lower than in 2018, while
364 meteorological conditions were comparable in both years. The significant year-to-year variability depended
365 presumably on the meteorological conditions, on new imposed regulations as well as on the fact that the CNY
366 period is determined with a lunar calendar and therefore the exact CNY period varies from year-to-year. In
367 2013, 2014, and 2015, haze episodes lasting several days were observed immediately following the CNY. In
368 2016 and 2018 a moderate haze episode began one day following the CNY.

369

370 Comparing the level of increase in pollutant concentrations during CNY night inside and outside Beijing 5th
371 ring road (firework prohibition area) revealed that in 2019 the increase inside this area was smaller than outside.
372 During most, but not all, of the previous CNYS, the increase in concentration was higher inside than outside.
373 This was also the case in 2018. However, as also in previous years the ratio of inside and outside concentrations
374 during CNY has varied, it is unclear if this is related to efficacy of the emission prohibition or, e.g., to larger
375 scale air-mass movements. As absolute concentrations, our results show a decrease of CNY pollution within
376 the prohibition area since 2016 and especially in 2019. This is in agreement with the previous Liu et al. 2019
377 study, which compared the 2016 and 2018 CNY (before and after the prohibition took effect).

378

379 This long-term analysis, which combines BUCT data with multiple years of Chinese government data,
380 demonstrates the importance of analyzing multiple data sources to determine overall trends, rather than making
381 conclusions based on a single dataset. This also demonstrates the usefulness of long-term measurements.
382 Therefore, we suggest ongoing measurements at both BUCT-AHL and MEP sites into multiple future years.



383

384 The combination of the BUCT-AHL comprehensive observations together with the spatial variability provided
385 by the MEP sites, we see excellent potential that can be utilized to investigate the changes in a) atmospheric
386 chemistry – like ozone dynamics and sulfuric acid formation; b) atmospheric gas-to-particle conversion; c)
387 boundary layer dynamics and d) air quality. Here we have investigated CNYs as case studies to get better
388 insight how rapid changes in emissions will affect the previous four items.

389

390 **ACKNOWLEDGEMENTS**

391

392 The work is supported by Academy of Finland via Center of Excellence in Atmospheric Sciences (project no.
393 272041) and European Research Council via ATM-GTP 266 (742206). This research has also received funding
394 from Academy of Finland (project no. 316114 & 315203, 307537), Business Finland via Megasense-project,
395 European Commission via SMart URBan Solutions for air quality, disasters and city growth, (689443), ERA-
396 NET-Cofund as well as the Doctoral Programme in Atmospheric Sciences at the University of Helsinki. Partial
397 support from the National Key R&D Program of China (2016YFC0200500), and the National Natural Science
398 Foundation of China (91544231 & 41725020) is acknowledged. The authors also wish to acknowledge the
399 Finnish Centre for Scientific Computing (CSC) – IT Center for Science, Finland, for computational resources.

400

401 **AUTHOR CONTRIBUTIONS**

402

403 All BUCT affiliated authors, plus KD, BC, YW, TC, and PR contributed to measurement collection at BUCT.
404 LW provided the quality-controlled MEP data. BF, LD, KD, TP, FB and MK conceptualized and conducted
405 the data analysis. TK, MoK, RP, and RB participated in the data analysis. TK and MoK provided the
406 meteorology data. KD, TP, FB, PP and MK supervised the study. BF visualized the data and visualized the data
407 and prepared the manuscript with contributions from all other authors. SG assisted with the data visualization
408 and generating figures.

409

410 **COMPETING INTERESTS**

411

412 The authors declare that there are no conflicts of interest in this study.

413

414 **REFERENCES**

415

416 Bach, W., Daniels, A., Dickinson, L., Hertlein, F., Morrows, J., Margolis, S., and Dinh, V. D. (2007). Fireworks
417 Pollution and Health. *International Journal of Environmental Studies*.7,1975:183-192.

418

419 Barman, S. C., Singh, R., Negi, M. P. S., and Bhargava, S. K. (2007). Ambient air quality of Lucknow City
420 (India) during use of fireworks on Diwali Festival. *Environ. Monit. Assess.*, 137:495–504.

421

422 Chen, B., Kan, H., Chen, R., Jiang, S., and Hong, C. (2011). Air Pollution and Health Studies in China—Policy
423 Implications. *Journal of the Air & Waste Management Association*.65-11:1292-1299.

424

425 Chou, C. C.-K., Tsai, C.-Y., Shiu, C.-J., Liu, S. C., and Zhu, T. (2009). Measurement of NO_y during Campaign
426 of Air Quality Research in Beijing 2006 (CAREBeijing-2006): Implications for the ozone production efficiency
427 of NO_x. *Journal of Geophysical Research: Atmospheres*. 114:D00G01.

428



- 429 Feng, J., Sun, P., Hu, X., Zhao, W., Wu, M., and Fu, J. (2012). The chemical composition and sources of pm_{2.5}
430 during the 2009 Chinese new year's holiday in Shanghai. *Atmospheric Research*, 118:435–444.
431
- 432 Hari, P. and Kulmala, M. (2005). Station for Measuring Ecosystem-Atmosphere Relations (SMEAR II). *Boreal*
433 *Environment Research*. 10:315-322.
434
- 435 He, H., Li, C., Loughner, C. P., Li, Z., Krotkov, N. A., Yang, K., Wang, W., Zheng, Y., Bao, X., Zhao, G., and
436 Dickerson, R. R. (2012). SO₂ over central China: Measurements, numerical simulations and the tropospheric
437 sulfur budget. *Journal of Geophysical Research*, 117, D00K37.
438
- 439 Heintzenberg, J., Wehner, B., and Birmili, W. (2007). ‘How to find bananas in the atmospheric aerosol’: new
440 approach for analyzing atmospheric nucleation and growth events. *Tellus B: Chemical and Physical*
441 *Meteorology*, 59:2, 273-282.
442
- 443 Jiang, Q., Sun, Y. L., Wang, Z., and Yin, Y. (2015). Aerosol composition and sources during the Chinese
444 Spring Festival: fireworks, secondary aerosol, and holiday effects. *Atmospheric Chemistry and Physics*,
445 15:6023–6034.
446
- 447 Kong, S. F., Li, L., Li, X. X., Yin, Y., Chen, K., Liu, D. T., Yuan, L., Zhang, Y. J., Shan, Y. P., Ji, Y. Q. (2015)
448 The impacts of firework burning at the Chinese Spring Festival on
449 air quality: insights of tracers, source evolution and aging processes. *Atmospheric Chemistry and*
450 *Physics*. 15:2167-2184.
451
- 452 Kulmala, M. (2015). Atmospheric Chemistry: China's Chocking Cocktail. *Nature Comment*.
453
- 454 Kulmala, M. (2018). Build a global Earth observatory. *Nature Comment*.
455
- 456 Kürten, A., Rondo, L., Ehrhart, S., and Curtius, J. (2012). Calibration of a chemical ionization mass
457 spectrometer for the measurement of gaseous sulfuric acid. *The Journal of Physical Chemistry A*. 116:6375-
458 6386.
459
- 460 Li, W., Shi, Z., Yan, C., Yang, L., Dong, C., and Wang, W. (2013). Individual metal-bearing particles in a
461 regional haze caused by firecracker and firework emissions. *Sci. Total Environ*, 443, 464-469.
462
- 463 Liu, D.-Y., Rutherford, D., Kinsey, M., and Prather, K. A. (1997). Real-Time Monitoring of Pyrotechnically
464 Derived Aerosol Particles in the Troposphere. *Analytical Chemistry*, 69, 1808-1814.
465
- 466 Liu, J. Q., Jiang, J. K., Zhang, Q., Deng, J. G., and Hao, J. M. (2016). A spectrometer for measuring particle
467 size distributions in the range of 3 nm to 10 μm, *Frontiers of Environmental Science & Engineering*, 10:63–
468 72.
469
- 470 Liu, J., Chen, Y., Chao, S., Cao, H., and Zhang, A. (2019). Levels and health risks of PM_{2.5}-bound toxic metals
471 from firework/firecracker burning during festival periods in response to management strategies. *Ecotoxicology*
472 *and Environmental Safety*. 171:406-413.
473
- 474 Liu, Y.C., Yan, C., Feng, Z., Zheng, F., Fan, X., Zhang, Y., Li, C., Zhou, Y., Lin, Z., Guo, Y., Zhang, Y., Ma,
475 L., Zhou, W., Liu, Z., Dada, L., Dällenbach, K., Kontkanen, J., Cai, R., Chan, T., Chu, B., Du, W., Yao, L.,



- 476 Wang, Y., Cai, J., Kangasluoma, J., Kokkonen, T., Kujansuu, J., Rusanen, A., Deng, C., Fu, Y., Yin, R., Li, X.,
477 Lu, Y., Liu, Y., Lian, C., Yang, D., Wang, W., Ge, M., Wang, Y., Worsnop, D.R., Junninen, H., He, H.,
478 Kerminen, V.-M., Zheng, J., Wang, L., Jiang, J., Petäjä, T., Bianchi, F. and Kulmala, M. (2020) Continuous
479 and comprehensive atmospheric observation in Beijing: a station to understand the complex urban atmospheric
480 environment, *Big Earth Data* 4, 295-321.
- 481
- 482 Manninen, H. E., Mirme, S., Mirme, A., Petäjä, T., and Kulmala, M. (2016). How to reliably detect molecular
483 clusters and nucleation mode particles with Neutral cluster and Air Ion Spectrometer (NAIS), *Journal of*
484 *Atmospheric Measurement Techniques*, 9:3577-3605, 10.5194/amt-9-3577-2016, 2016.
- 485
- 486 Mirme, S., and Mirme, A. (2013) The mathematical principles and design of the NAIS – a spectrometer for the
487 measurement of cluster ion and nanometer aerosol size distributions. *Journal of Atmospheric Measurement*
488 *Techniques*, 6:1061-1071, 2013.
- 489
- 490 Mönkkönen, P., Koponen, I.K., Lehtinen, K.E.J., Uma, R., Srinivasan, D., Hämeri, K., and Kulmala, M. (2004).
491 Death of nucleation and Aitken mode particles: observations at extreme atmospheric conditions and their
492 theoretical explanation. *Journal of Aerosol Science*. 35:781-787.
- 493
- 494 Peltonen, M. (2017). University of Helsinki builds an air quality measuring station in Beijing. *University of*
495 *Helsinki News and Press Releases*.
- 496
- 497 Ravindra, K., Mor, S., and Kaushik, C. P. (2003). Short-term variation in air quality associated with firework
498 events: A case study. *Journal of Environ. Monit.*, 5. 260–264.
- 499
- 500 Shen, X. J., Sun, J. Y., Zhang, Y.M., Wehner, B., Nowak, A., Tuch, T., Zhang, X. C., Wang, T. T., Zhou, H.
501 G., Zhang, X. L., Dong, F., Birmili, W., and Wiedensohler, A. (2011). First long-term study of particle number
502 size distributions and new particle formations of regional aerosol in the North China Plain. *Atmospheric*
503 *Chemistry and Physics*, 11:1565-1580.
- 504
- 505 Shi, G.-L., Liu, G.-R., Tian, Y.-Z., Zhou, X.-Y., Peng, X., and Feng, Y.-C. (2014). Chemical characteristic and
506 toxicity assessment of particle associated PAHs for the short-term anthropogenic activity event: During the
507 Chinese new year's festival in 2013. *Science of the Total Environment*, 482-483:8–14.
- 508
- 509 Singh, D. P., Gadi, R., Mandal, T.K., Dixit, C.K., Singh, K., Saud, T., Singh, N., and Gupta, P. K. (2009).
510 Study of temporal variation in ambient air quality during Diwali festival in India. *Environ. Monit. Assess.*
511 169:1–13.
- 512
- 513 Song, C., Wu, L., Xie, Y., He, J., Chen, X., Wang, T., Lin, Y., Jin, T., Wang, A., Liu, Y., Dai, Q., Liu, B.,
514 Wang, Y., and Mao, H. (2017). Air pollution in China: Status and spatiotemporal variations. *Environmental*
515 *Pollution*. 227:334-347.
- 516
- 517 Tao, M., Chen, L., Li, R., Wang, L., Wang, J., Wang, Z., Tang, G., and Tao, J. (2016). Spatial Oscillation of
518 the particle pollution in eastern China during winter: Implications for regional air quality and climate.
519 *Atmospheric Environment*.144:100-110.
- 520



- 521 van der A, R. J., Mijling, B., Ding, J., Koukouli, M. E., Liu, F., Li, Q., Mao, H., and Theys, N. (2017) Cleaning
522 up the air: effectiveness of air quality policy for SO₂ and NO_x emissions in China, *Atmospheric Chemistry and*
523 *Physics*, 17:1775-1789.
- 524
- 525 Vanhanen, J., Mikkilä, J., Lehtipalo, K., Sipilä, M., Manninen, H. E., Siivola, E., Petäjä, T., and Kulmala, M.
526 (2011). Particle Size Magnifier for Nano-CN Detection. *Aerosol Science and Technology*, 45:533-542,
527 10.1080/02786826.2010.547889.
- 528
- 529 Virkkula, A., Chi1, X., Ding, A., Shen, Y., Nie, W., Qi, X., Zheng, L., Huang, X., Xie, Y., Wang, J., Petäjä,
530 T., and Kulmala, M. (2015). On the interpretation of the loading correction of the aethalometer. *Atmospheric*
531 *Measurement Techniques*. 8:4415–4427.
- 532
- 533 Xue, W., Wang, J., Niu, H., Yang, J., Han, B., Lei, Y., Chen, H., and Jiang, C. (2013). Assessment of air quality
534 improvement effect under the National Total Emission Control Program during the Twelfth National Five-Year
535 Plan in China. *Atmospheric Environment*. 68:74-81.
- 536
- 537 Wu, H. J., Tang, X., Wang, Z. F., Wu, L., Lu, M. M., Wei, L. F., and Zhu, J. (2018). Probabilistic automatic
538 outlier detection for surface air quality measurements from the China National Environmental Monitoring
539 Network. *Adv. Atmos. Sci.*, 35(12), 1522–1532.
- 540
- 541 Yang, L., Gao, X., Wang, X., Nie, W., Wang, J., Gao, R., Xu, P., Shou, Y., Zhang, Q., and Wang, W. (2014).
542 Impacts of firecracker burning on aerosol chemical characteristics and human health risk levels during the
543 Chinese New Year celebration in Jinan, China. *Science of the Total Environment*, 476-477:57–64.
- 544
- 545 Yerramsetti, V. S., Anu Rani Sharma, A. R., Navlur, N. G., Rapolu, V., Chitanya Dhulipala, N. S. K. C., and
546 Sinha, P. R. (2013). The impact assessment of Diwali fireworks emissions on the air quality of a tropical urban
547 site, Hyderabad, India, during three consecutive years. *Environ. Monit. Assess.*, 185:7309–7325.
- 548
- 549 Zhang, M., Wang, X., Chen, J., Cheng, T., Wang, T., Yang, X., Gong, Y., Geng, F., and Chen, C. (2010).
550 Physical characterization of aerosol particles during the Chinese new year's firework events. *Atmospheric*
551 *Environment*, 44:5191–5198.
- 552
- 553 Zhao, X., Zhang, X., Pu, W., Meng, W., Xu, X. (2011). Scattering properties of the atmospheric aerosol in
554 Beijing, China. *Atmospheric Research*. 101:799-808.
- 555
- 556 Zhao, X. J., Zhao, P. S., Xu, J., Meng, W., Pu, W. W., Dong, F., He, D., Shi, Q. F. (2013). Analysis of a winter
557 regional haze event and its formation mechanism in the North China Plain. *Atmospheric Chemistry and Physics*.
558 13:5685-5696.
- 559
- 560 Zhou, Y., Dada, L., Liu, Y., Fu, Y., Kangasluoma, J., Chan, T., Yan, C., Chu, B., Daellenbach, K. R., Bianchi,
561 F., Kokkonen, T. V., Liu, Y., Kujansuu, J., Kerminen, V.-M., Petäjä, T., Wang, L., Jiang, J., and Kulmala, M.
562 (2020). Variation of size-segregated particle number concentrations in wintertime Beijing. *Atmospheric*
563 *Chemistry and Physics*. 20:1201–1216
- 564



565

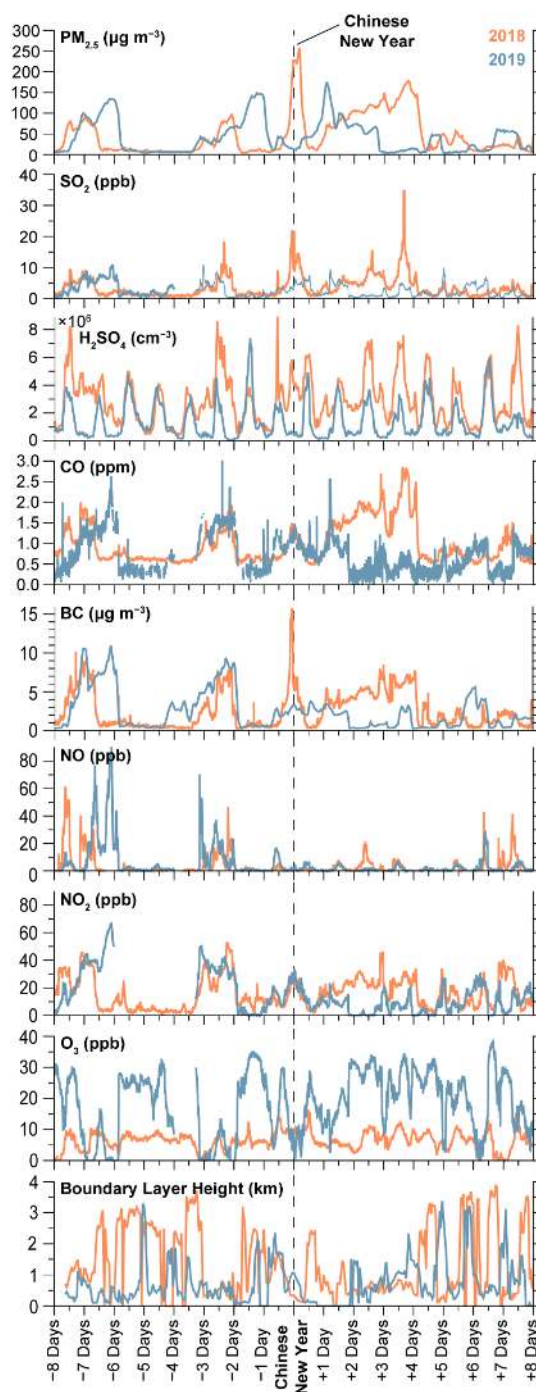


566

567

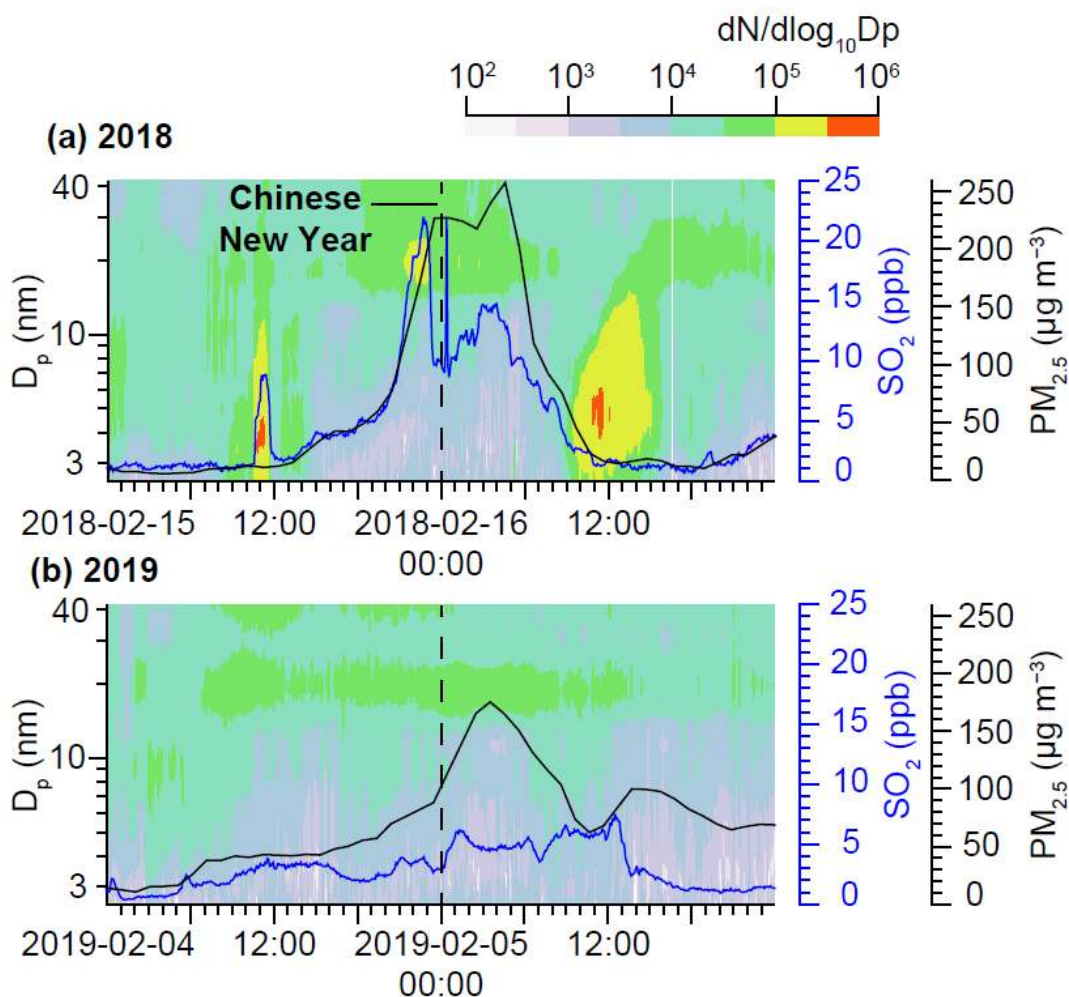
568 **Figure 1:** Location of the BUCT-AHL site within the Beijing metropolitan area. © OpenStreetMap
569 contributors, CC BY-SA.

570



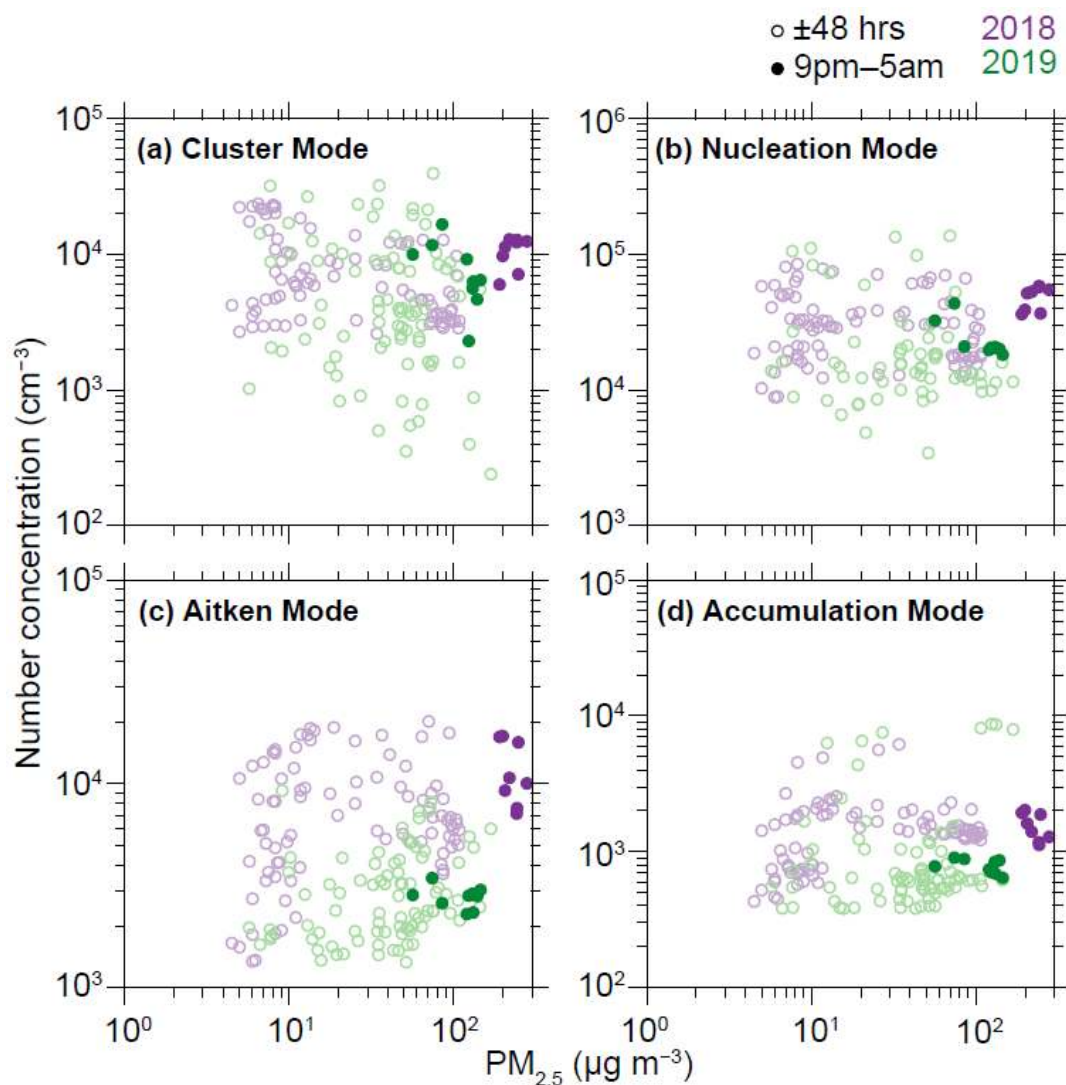
571
572

Figure 2: Major pollutants measured in Beijing during the 2018 and 2019 CNY.



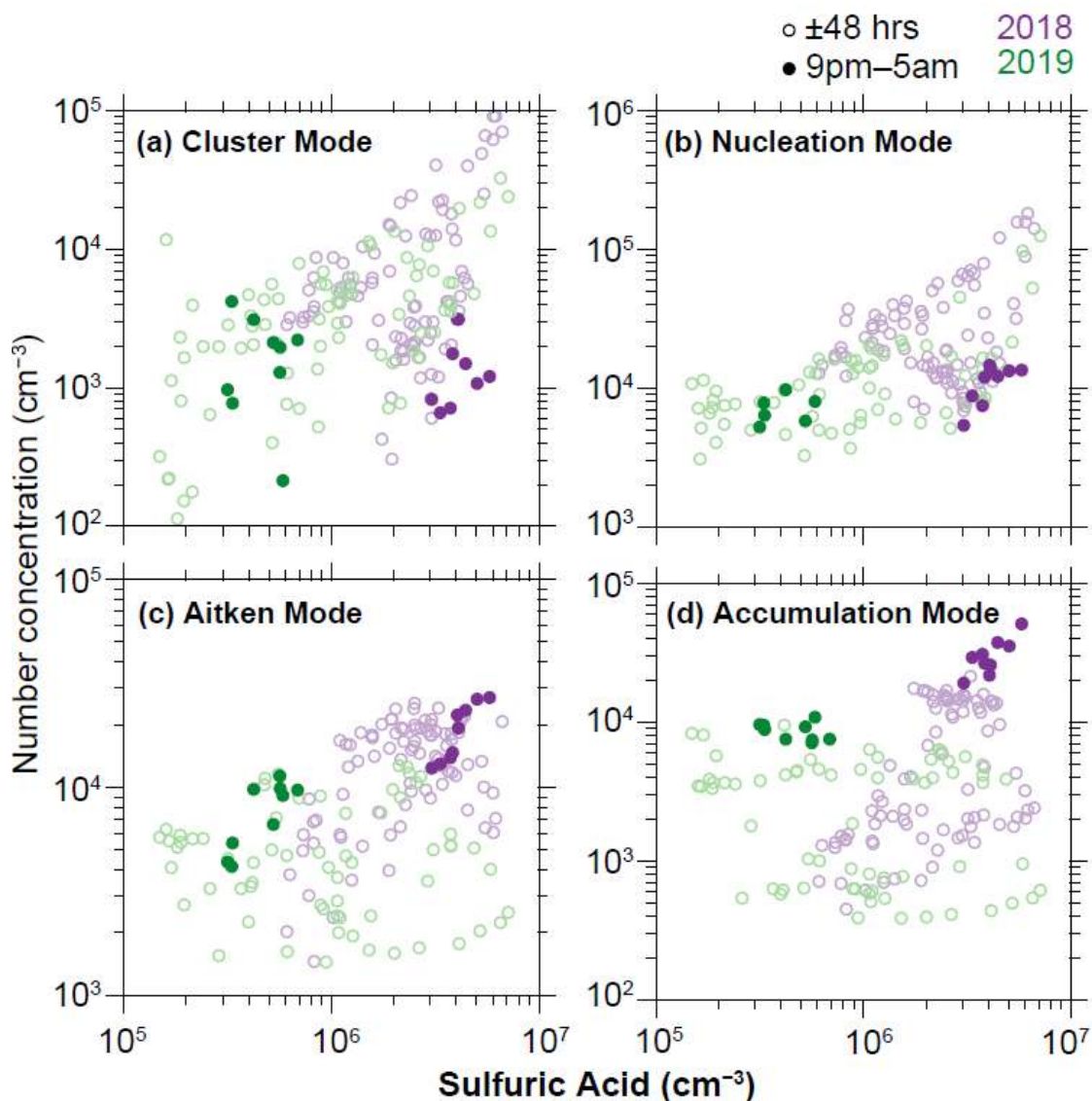
573
574
575
576
577
578

Figure 3: Aerosol number size distribution from NAIS instrument from one day before the CNY through one day following the CNY in 2018 and 2019, overlain with aerosol mass concentration $PM_{2.5}$ (black lines) and SO_2 (blue lines). A spike of $PM_{2.5}$ and SO_2 is observed in both years, but significantly less in 2019. Results from the NAIS show a corresponding release of particles approximately 11 nm in diameter during the time of the CNY fireworks.



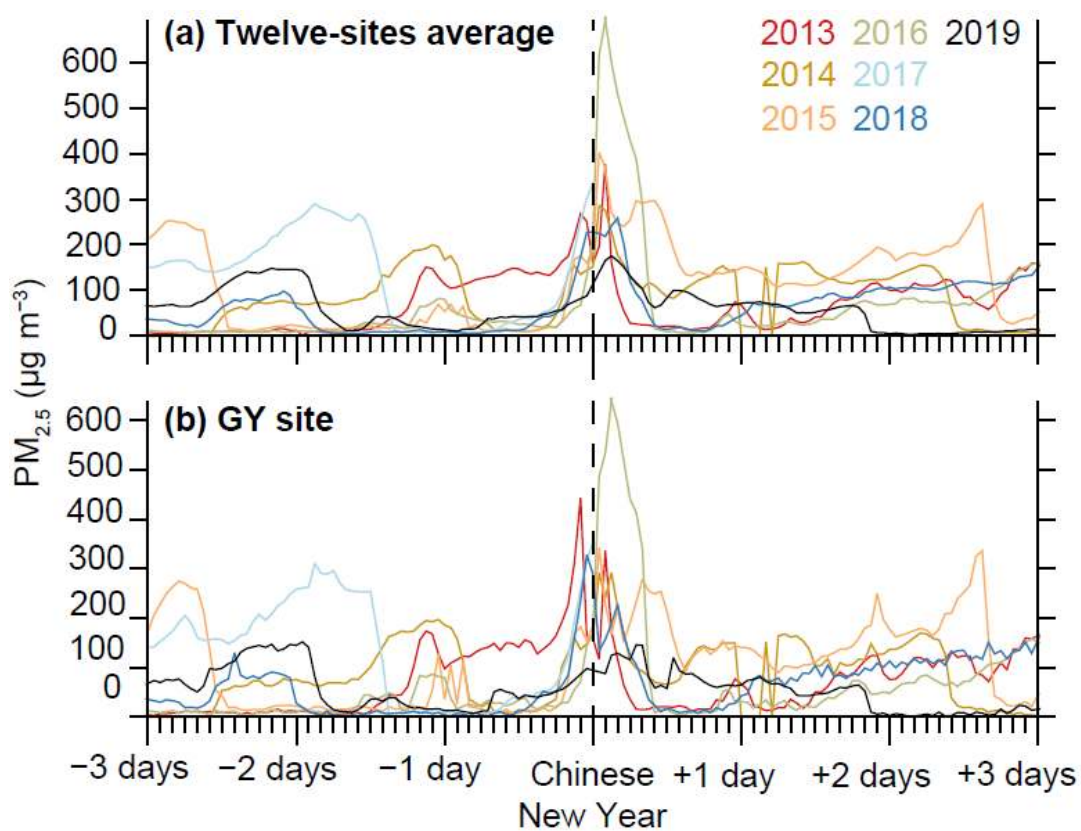
579
580
581
582
583

Figure 4: PM_{2.5} number concentration as a function of mass concentration in cluster, nucleation, Aitken, and accumulation modes in 2018 and 2019, with comparison of CNY ± 48 hours with measurements from 9pm through 5am the night of the CNY. Measurements are from BUCT-AHL.



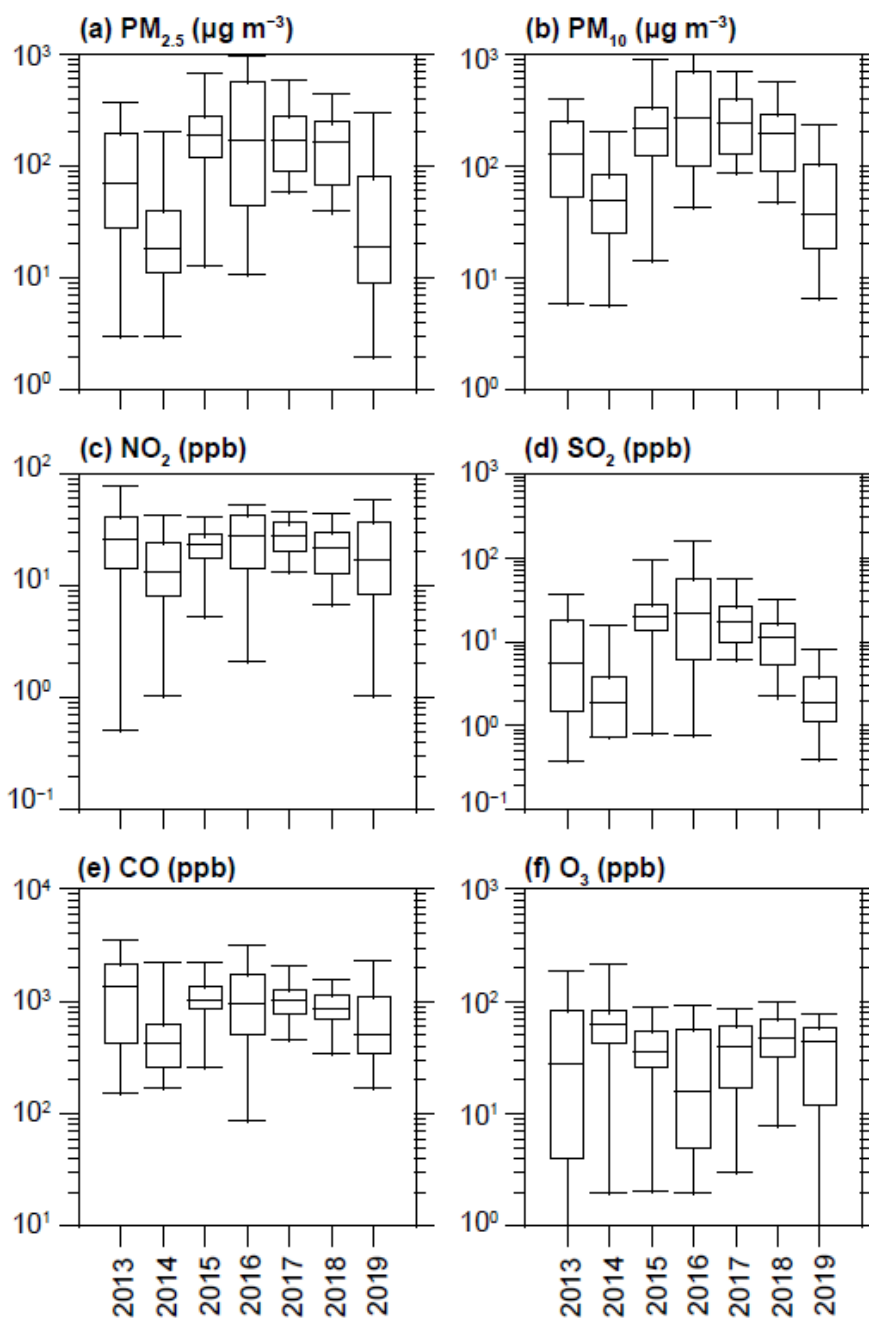
584
585
586
587
588

Figure 5: Number concentration of particles in cluster, nucleation, Aitken, and accumulation modes as a function of sulfuric acid concentration in 2018 and 2019, with comparison of CNY \pm 48 hours with measurements from 9pm through 5am the night of the CNY. Measurements are from BUCT-AHL.



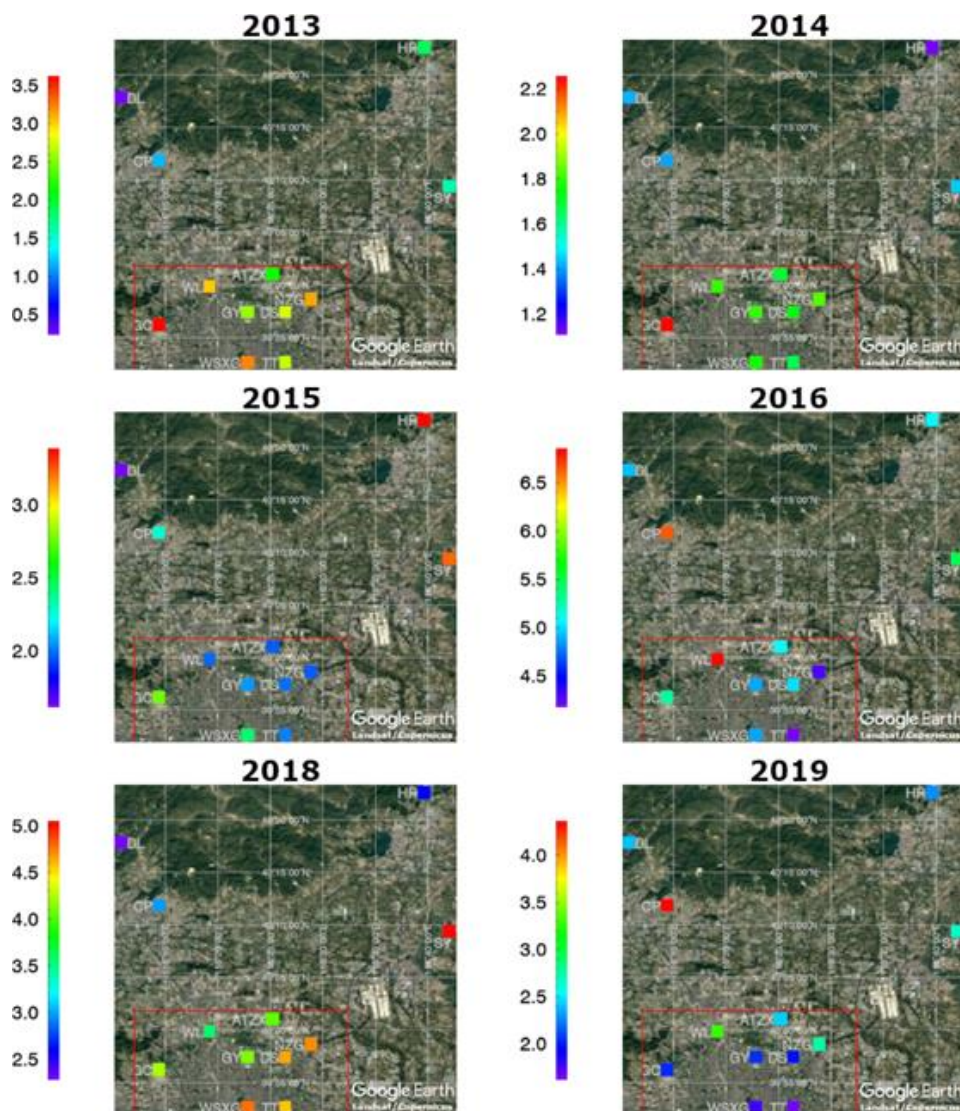
589
590
591
592
593
594

Figure 6: PM_{2.5} averaged from 12 MEP sites in Beijing (top) and from only the Guanyuan (GY) site, which is the closest MEP measurement site to BUCT-AHL (bottom), from three days before through three days after the 2013-2019 CNY. The highest peak of pollution during the CNY overnight was in 2016, and the lowest was in 2019.

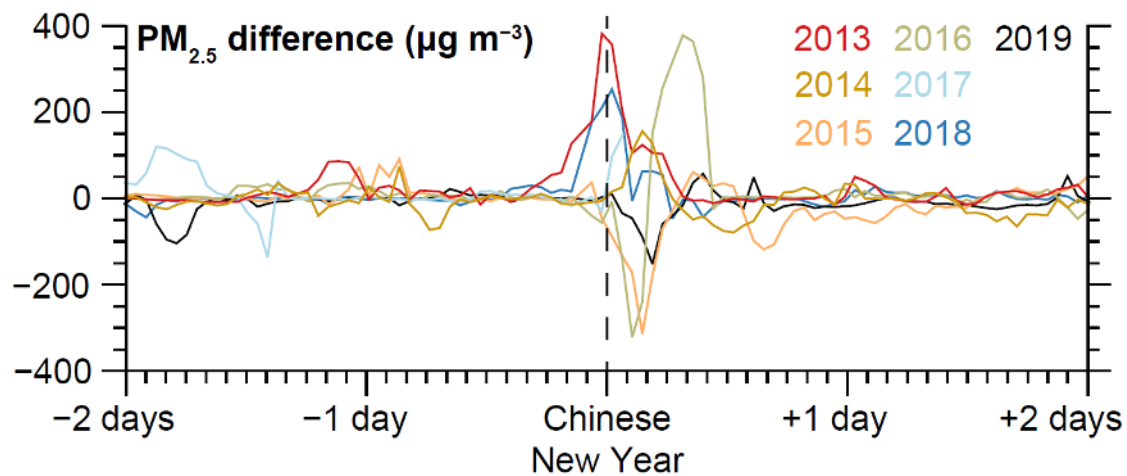


595
596
597
598
599

Figure 7: Boxplots of particulate matter and trace gases between 18:00 and 06:00 on the night of the Chinese New Year in the years 2013-2019. boxplots show 1st, 25th, 50th, 75th, and 99th percentiles of the data across the 12 sites during this 12-hour period (13 time points, inclusively).



600
601 **Figure 8:** The 12 MEP sites mapped in the Beijing metropolitan area, showing the ratio of overnight $PM_{2.5}$
602 observations during the CNY (21:00-05:00) to all data during the period of 48 hours before through 48 hours
603 after the CNY. The red line marks the approximate location of the 5th Ring Road. Note that the colorbars in
604 each map are relative to only that year, and the colorbar range is not the same in different years. 2017 is omitted
605 from this figure because data after 00:00 was not available. © Google Earth
606



607
608
609
610

Figure 9: Differences of $PM_{2.5}$ inside vs. outside the 5th Ring Road of Beijing from 2013 through 2019.